

Physics-Based Analysis and Simulation of $1/f$ Noise in MOSFETs Under Large-Signal Operation

Sung-Min Hong, *Member, IEEE*, Chan Hyeong Park, *Member, IEEE*,
Young June Park, *Senior Member, IEEE*, and Hong Shick Min

Abstract—This paper presents a study on $1/f$ noise in MOSFETs under large-signal (LS) operation, which is important in CMOS analog and RF integrated circuits. The flicker noise is modeled with noise sources as a perturbation in the semiconductor equations employing McWhorter's oxide-trapping model and Hooge's empirical $1/f$ noise model. Numerical results are shown for $1/f$ noise in the MOSFET in both small-signal operation and periodic LS operation. It is shown that McWhorter's model does not give any significant $1/f$ noise reduction when the oxide traps are distributed uniformly in energy and space. In contrast, Hooge's model gives almost 6-dB $1/f$ noise reduction as the gate OFF-voltage decreases below the threshold voltage. It is found that both models fall short of explaining the noise reduction by more than 6 dB, as observed experimentally in the literature. However, when only one active oxide trap is considered, which generates random telegraph signal (RTS) in drain current, the LS operation gives more than 6-dB low-frequency RTS noise reduction.

Index Terms—Cyclostationary noise, Hooge's empirical $1/f$ noise model, McWhorter's oxide-trapping model, $1/f$ noise in MOSFETs.

I. INTRODUCTION

FOR the analysis and design of CMOS analog and RF integrated circuits, $1/f$ noise in MOSFETs is one of the factors limiting the achievable dynamic range of electronic MOS circuits. For example, $1/f$ noise has been known as the major cause of close-in phase noise in CMOS RF oscillators [1].

The analysis and characterization of $1/f$ noise in MOSFETs is typically performed for MOSFETs in the small-signal operation, where only dc biases are imposed on the device electrodes.

Manuscript received October 26, 2009; revised January 25, 2010. First published March 1, 2010; current version published April 21, 2010. This work was supported by the National Core Research Center program of KOSEF through the NANO Systems Institute at Seoul National University, by the Brain Korea 21 Project, and Samsung Electronics Company under Grants 0414-20050009 and 0414-20050037. The work of S.-M. Hong was supported in part by a Korea Research Foundation Grant by the Korean Government (MOEHRD) under Contract KRF-2007-357-D00159. The work of C. H. Park was supported by the Korean Government (MEST) through the National Research Foundation of Korea (NRF) under Grant 2009-0076872 and was conducted under the research grant of Kwangwoon University in 2008. The review of this paper was arranged by Editor M. J. Deen.

S.-M. Hong is with the Institute for Microelectronics and Circuit Theory (EIT4), Bundeswehr University, 85577 Neubiberg, Germany.

C. H. Park is with the Department of Electronics and Communications Engineering, Kwangwoon University, Seoul 139-701, Korea (e-mail: chan-park@kw.ac.kr).

Y. J. Park and H. S. Min are with the School of Electrical Engineering and Computer Science and the Nano System Institute, National Core Research Center (NSI-NCRC), Seoul National University, Seoul 151-744, Korea.

Color versions of one or more of the figures in this paper are available online at <http://ieeexplore.ieee.org>.

Digital Object Identifier 10.1109/TED.2010.2043186

Experimental results [2]–[4], however, show that the estimates based on the small-signal $1/f$ noise model can be inaccurate, particularly for the periodically switched MOSFETs. It was shown that the measured power spectral density of the drain noise voltage (or current) is much lower than the estimate using the small-signal $1/f$ noise model, i.e., 6-dB noise power reduction. Although modeling efforts to explain and predict these observed effects [5], [6] have been made, the physics-based analysis and simulation of $1/f$ noise in MOSFETs has been performed only in the small-signal operation regime [7], [8]. To our knowledge, its extension to the periodic large-signal (LS) operation has not been reported yet.

In this paper, we calculate the power spectral density of the drain $1/f$ noise current in the MOSFET in periodic LS operation by using both the oxide-trapping model [7], [9] and Hooge's model [10]–[12]. This paper is organized as follows: In Section II, we briefly describe the implementation of the physics-based simulation of $1/f$ noise in the MOSFET using both the oxide-trapping model and Hooge's empirical relation. In Section III, numerical results and their discussions are given for the MOSFET in the periodic LS as well as in the small-signal operation. The conclusion is given in Section IV.

II. PHYSICS-BASED ANALYSIS AND SIMULATION OF $1/f$ NOISE IN MOSFET

In spite of extensive studies for nearly half a century, the physical origin of $1/f$ noise in MOSFETs has not been unambiguously understood [12], [13]. However, it is widely accepted that the sources of $1/f$ noise in MOSFETs are located at or near the Si/SiO₂ interface. At present, there exist two theories on the physical origin of $1/f$ noise in MOSFETs: 1) the carrier number fluctuation theory based on the oxide-trapping model [7], [9], [14] and 2) the mobility fluctuation theory based on Hooge's well-known empirical relation [10]–[12].

Here, we employ both McWhorter's oxide-trapping noise model and Hooge's empirical $1/f$ noise model to compare their simulation results on $1/f$ noise under LS operation as a platform for our simulation study. We choose an NMOSFET as a basis of our discussion, but its application to PMOSFETs is straightforward.

A. McWhorter's Oxide-Trapping Model

Fig. 1 shows the energy band diagram that illustrates possible carrier transition processes at the interface and in the oxide, which is considered for the McWhorter $1/f$ noise model in this

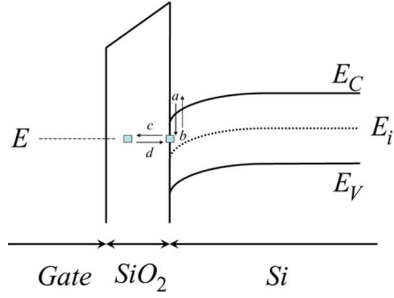


Fig. 1. Energy band diagram that illustrates possible carrier transition processes at the interface and in the oxide. Only traps with energy E are depicted.

study. Electrons in the conduction band can get trapped into (process a) or detrapped from (process b) the localized defect centers at the interface. The trapped electrons at the interface can also get captured or emitted with defect centers in the oxide that have the same energy through the tunneling mechanism (processes c and d).

Let us consider oxide traps with energy level E , whose volume density is $N_{t,ox}$. $N_{t,int}$ denotes the sheet density of the interface traps that can exchange electrons with the oxide traps with the same energy E . In addition, $n_{t,ox}$ and $n_{t,int}$ represent the trapped electron volume density in the oxide traps and the trapped electron sheet density in the interface traps, respectively. The expressions characterizing the processes a , b , c , and d in Fig. 1 respectively become

$$r_{n,int} = c_n n (N_{t,int} - n_{t,int}) \quad (1)$$

$$g_{n,int} = c_n n_{t,int} n_1 \quad (2)$$

$$r_{int,ox} = T n_{t,int} \Delta x (N_{t,ox} - n_{t,ox}) \quad (3)$$

$$g_{int,ox} = T (N_{t,int} - n_{t,int}) n_{t,ox} \Delta x. \quad (4)$$

Note that the four quantities $r_{n,int}$, $g_{n,int}$, $r_{int,ox}$, and $g_{int,ox}$ have the unit of $\text{cm}^{-2} \text{sec}^{-1}$. In (1)–(4), n is the electron volume density in the conduction band at the interface, c_n is the capture coefficient for electrons, n_1 is the Shockley density, which is the electron density when the electron quasi-Fermi energy is equal to E , and T is the tunneling coefficient with the unit of $\text{cm}^2 \text{sec}^{-1}$. The electron continuity equation, the interface trap continuity equation, and the oxide trap continuity equation can respectively be written as

$$\int_{\Omega_{int}} d\mathbf{a} \cdot \mathbf{J}_n = q \int_{A_{int}} da (r_{n,int} - g_{n,int}) + q \int_{\Omega_{int}} d\mathbf{r} \frac{\partial}{\partial t} n \quad (5)$$

$$0 = q \int_{A_{int}} da \left(\frac{\partial}{\partial t} n_{t,int} - r_{n,int} + g_{n,int} + r_{int,ox} - g_{int,ox} \right) \quad (6)$$

$$0 = q \int_{\Omega_{ox}} d\mathbf{r} \frac{\partial}{\partial t} n_{t,ox} + q \int_{A_{int}} da (-r_{int,ox} + g_{int,ox}). \quad (7)$$

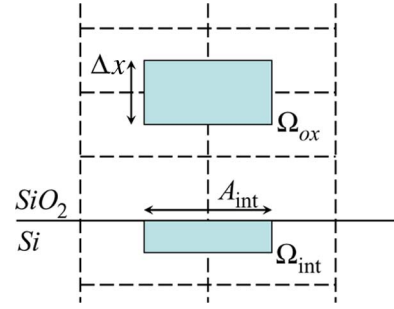


Fig. 2. Spatial discretization of the MOSFET. Ω_{int} is the control volume whose surface includes the interface, A_{int} is the area of the interface, and Ω_{ox} is the control volume of the oxide node where the oxide trap is located.

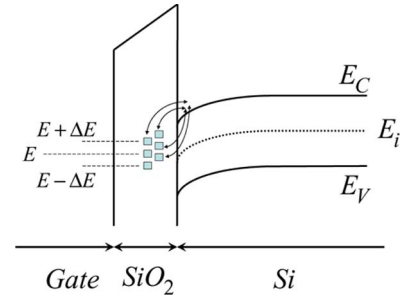


Fig. 3. Energy band diagram that illustrates the direct transitions between the conduction band and the oxide traps under the quasi-static assumption of $n_{t,int}$. We discretize the selected energy range in the oxide bandgap in small discrete energy interval ΔE .

In (5)–(7), Ω_{int} and Ω_{ox} are the control volumes, and A_{int} is the interface area, as shown in Fig. 2.

Since the trap centers at the interface and in the oxide are distributed in energy and space, discretization in both variables is needed. In the previous study on the physics-based simulation of $1/f$ noise in MOSFETs [7], only the trap levels at the electron quasi-Fermi level were discretized, mainly due to the computational efficiency. This approach can be valid only when the electron quasi-Fermi level of the oxide traps is aligned with that of the interface traps. However, when the MOSFET is switched periodically, this assumption is no longer valid, as shown in the following section, because the electron trapping and detrapping by the oxide traps, which are related with $1/f$ noise in the oxide-trapping model, are known to be slow processes compared with the switching frequency.

Therefore, in this paper, we discretize the selected energy range in the oxide bandgap with small discrete energy interval ΔE to account for the trap states that are related with $1/f$ noise under LS excitation condition, as shown in Fig. 3. Although this implementation is computationally expensive, we expect that it gives more accurate results. Instead, we make the following assumption to reduce the computational complexity. Since the time constant for the interface trap is much shorter than that of the oxide trap [7], [9], [15], the quasistatic approximation on $n_{t,int}$ can be made as

$$\frac{\partial}{\partial t} n_{t,int} = 0. \quad (8)$$

Through this simplification, we can consider the transitions of electrons between the conduction band and the oxide traps to

be direct without the intermediate interface states

$$\begin{aligned} \int_{\Omega_{\text{int}}} d\mathbf{a} \cdot \mathbf{J}_n &= q \int_{A_{\text{int}}} da (r_{\text{int,ox}} - g_{\text{int,ox}}) \\ &+ q \int_{\Omega_{\text{int}}} d\mathbf{x} \frac{\partial}{\partial t} n + q\gamma \quad (9) \\ 0 &= q \int_{\Omega_{\text{ox}}} d\mathbf{x} \frac{\partial}{\partial t} n_{t,\text{ox}} \\ &+ q \int_{A_{\text{int}}} da (-r_{\text{int,ox}} + g_{\text{int,ox}}) - q\gamma. \quad (10) \end{aligned}$$

Since we calculate the self-consistent solution of Poisson's equation and the continuity equations, the effect of the trapped electron in the oxide trap on the electrons in the channel is self-consistently included in our simulation results. Note that the nonlocal white noise source γ appears in the above continuity equations. Its correlation function can be expressed as follows:

$$R_{\gamma,\gamma}(t, t') = (r_{\text{int,ox}} + g_{\text{int,ox}}) \delta(t - t'). \quad (11)$$

The relevant transfer functions for this noise source are Green's functions for the oxide trap continuity equation and the electron continuity equation.

B. Hooge's Empirical Relation

Hooge's empirical relation [10]–[12] reads

$$S_{I,I} = \frac{\alpha_H}{f} \frac{I^2}{N} \quad (12)$$

where all the physical mechanisms related with the noise are contained in Hooge's parameter α_H . A phenomenological local colored (frequency-dependent) noise source ξ_n is superimposed in the current density. The continuity equation for the conduction band electron can be written as

$$\nabla \cdot (\mathbf{J}_n + \xi_n) = q \frac{\partial n}{\partial t}. \quad (13)$$

The relevant transfer function for Hooge's noise source is the gradient of Green's function for the electron continuity equation. The power spectral density of Hooge's noise source can be written as

$$S_{\xi_n, \xi_n}(\mathbf{r}, \mathbf{r}', f) = \frac{\alpha_H(\mathbf{r})}{f} \frac{|\mathbf{J}_{n,s}(\mathbf{r})|^2}{n(\mathbf{r})} \delta(\mathbf{r} - \mathbf{r}') I \quad (14)$$

where $\mathbf{J}_{n,s}$ is the steady-state electron current density, and I is a unit tensor.

Since Hooge's noise source is colored, its extension to the LS operation regime is not straightforward. We assume that Hooge's parameter is an instantaneous function. According to the scheme where frequency modulation is followed by amplitude modulation [16], we can find that the diagonal component

of the sideband correlation matrix [17]–[19] for Hooge's noise source is given by

$$S_{\xi_n, \xi_n}(\mathbf{r}, \mathbf{r}', mf_0 + f, mf_0 + f) = |K_m(\mathbf{r})|^2 \frac{1}{f} \delta(\mathbf{r} - \mathbf{r}') I \quad (15)$$

where $K_m(\mathbf{r})$ is the m th Fourier coefficient of $\alpha_H(\mathbf{r})(|\mathbf{J}_{n,s}(\mathbf{r})|^2/n(\mathbf{r}))$.

III. NUMERICAL RESULTS

Both McWhorter's oxide-trapping model and Hooge's empirical model, described in the previous section, have been implemented in our in-house device-circuit mixed-mode simulator Circuit LEvel SIMulation COde [20], [21].

To perform the physics-based noise simulation, we should first find the steady-state solutions—dc solutions or periodic LS solutions—without the influence of the noise sources. In the case of small-signal noise simulation, the dc solutions can be obtained easily by using the conventional dc simulation. In the case of the LS noise simulation, the periodic LS solutions can be obtained by using the periodic steady-state analysis methods, such as the finite-difference method [22], [23], the harmonic balance method [24], [25], or the shooting-Newton method [21], [26]. In this paper, the harmonic balance method has been exploited to be consistent with the following noise simulation. For the LS noise simulation, we employ the conversion Green's function technique that extends Green's function method for steady-state noise calculation into periodic steady-state noise calculation [17], [19], [20], [27], [28]. In the case of the LS analysis, the number of unknown variables used in the numerical procedure is significantly increased with the number of harmonics (or the number of discretized time points) considered in the simulation when compared with that in the case of small-signal analysis. Such a large linearized system equation is solved with ILUPACK, which is an efficient sparse matrix solver [29].

To illustrate the main differences that originated from two noise models, a long-channel MOSFET structure is chosen as the device under test. For such a device, a clear $1/f$ noise reduction by more than 6 dB has been observed experimentally under the switched operation with 50% duty cycle [2]–[4]. Application to more scaled devices can be an interesting topic and will be dealt with elsewhere.

A. Small-Signal Operation With Oxide-Trapping Model

We first calculate the $1/f$ noise spectrum using the oxide-trapping model when the MOSFET is in the small-signal operation.

Fig. 4 shows the cross-sectional view of the MOSFET under simulation. The gate contact is located from $-1.0 \mu\text{m}$ to $1.0 \mu\text{m}$ in the lateral position. The Si-SiO₂ interface is located at zero point in the vertical position. The thickness of the gate oxide is 9.0 nm. The threshold voltage of the MOSFET is calculated to be about 0.5 V. We consider the oxide trap levels beneath the gate contact, which are spatially located within 2.0 nm from the interface. The device width is $1.0 \mu\text{m}$. The unified

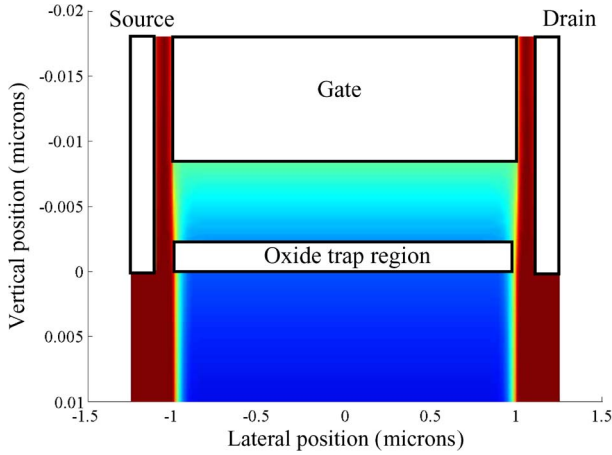


Fig. 4. Cross-sectional view of the MOSFET under simulation. The gate contact is located from -1.0 to $1.0 \mu\text{m}$ in the lateral position. The zero point in the vertical position is the oxide-silicon interface. The thickness of the gate oxide is 9.0 nm . The threshold voltage of the MOSFET is 0.5 V . The “oxide trap region” box indicates the region where the oxide trap levels are discretized. The device width is $1.0 \mu\text{m}$.

mobility model proposed by Darwish *et al.* [30] is adopted, and its dependence on the electric field is correctly considered.

The oxide trap density per unit volume and per unit energy at the trap energy E_t , i.e., $N_{t,\text{ox}}(E_t)$, may be modeled as a U-shaped distribution [31], [32] as

$$N_{t,\text{ox}}(E_t) = N_0 \exp[\eta \times (E_t - E_i)] \quad (16)$$

where N_0 and η are the fitting parameters, and E_i is the intrinsic energy level of silicon. The modeling of the oxide trap density has a significant impact on the noise simulation result. For example, in [33], the $1/f$ noise reduction under the switched operation observed in the experiments is attributed to this U-shaped distribution. In this paper, we consider two parameter sets: one is the usual U-shaped distribution taken from the literature [7], [31], [32], whereas the other is the uniform distribution originally assumed in McWhorter’s oxide-trapping model. The actual values used in the simulations are $N_0 = 4 \times 10^{17} \text{ cm}^{-3} \text{ eV}^{-1}$ and $\eta = 3.1 \text{ eV}^{-1}$ for the U-shaped distribution and $N_0 = 4 \times 10^{17} \text{ cm}^{-3} \text{ eV}^{-1}$ and $\eta = 0$ for the uniform distribution.

We consider oxide trap levels whose E_t values, measured from the electron quasi-Fermi level at the reference bias condition, are from -0.45 to 0.15 eV . The electron quasi-Fermi level is self-consistently determined under the presence of oxide trap levels. For that energy range, we introduce 25 discretized energy levels with the energy interval $\Delta E = 25 \text{ meV}$. Since there are 600 spatial nodes in the “oxide trap region” in Fig. 4, we need 15 000 additional unknown variables for the oxide traps. After the trap energy is determined self-consistently with the electron quasi-Fermi level at the reference bias condition, i.e., when the MOSFET is under the LS operation, the relative position in the energy band diagram of an oxide trap depends on the bias condition.

The tunneling coefficient T is given by

$$T = T_0 \exp(-\alpha|x|) \quad (17)$$

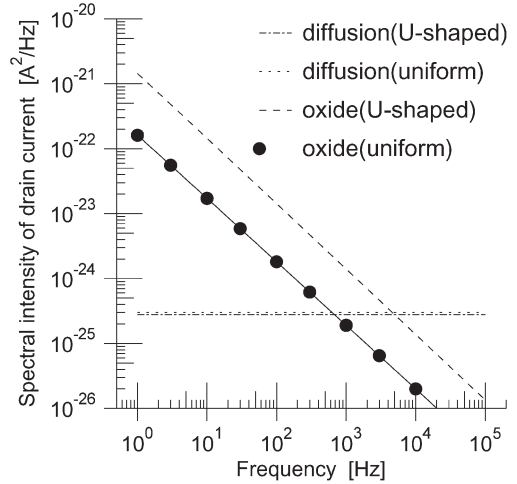


Fig. 5. Simulated power spectral densities of the drain noise current at the gate voltage 1.0 V as a function of frequency. The drain voltage is fixed to be 10 mV . The flat lines indicate the power spectral densities due to the diffusion noise sources.

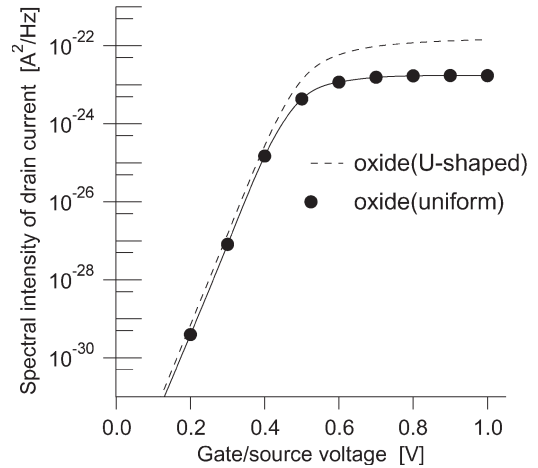


Fig. 6. Simulated power spectral densities of the drain noise current at 10 Hz as a function of gate voltage. Two different distributions of the oxide trap are considered. The drain voltage is fixed to be 10 mV . When the gate voltage is below the threshold voltage, which is 0.5 V for this simulation, the power spectral density of the drain noise current is much smaller than that of strong inversion.

where x is the depth of the oxide trap from the interface, T_0 is set to be $1.0 \text{ cm}^2 \text{ sec}^{-1}$, and the attenuation constant α is calculated using the trapezoidal barrier approximation. Therefore, the Jacobian matrix contains nonlocal components. Note that the validity of the simple square barrier approximation is doubtful under the LS operation since the barrier height depends on the bias condition. The interface trap density per unit energy is set to be $10^{11} \text{ cm}^{-2} \text{ eV}^{-1}$.

Fig. 5 shows the simulated power spectral densities of the drain noise current at the gate voltage of 1.0 V as a function of frequency. The drain voltage is fixed to be 10 mV . As expected, the oxide-trapping noise shows a clean $1/f$ noise spectrum. The change of slope due to the nonuniform trap distribution is negligible in the simulation. Fig. 6 shows the simulated power spectral densities of the drain noise current at 10 Hz as a function of gate voltage. When the gate voltage is below the threshold voltage, i.e., 0.5 V for this simulation, the power

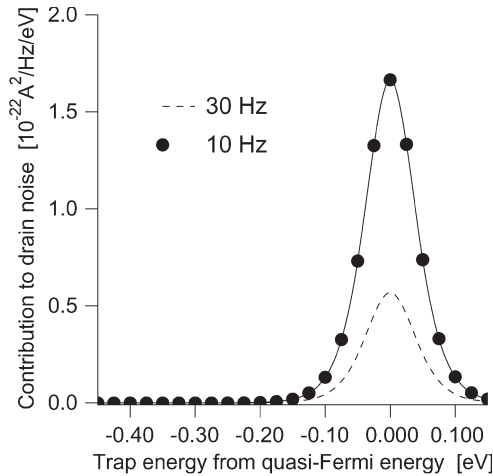


Fig. 7. Contribution of each trap with different energy to the power spectral density of the drain noise current at the gate voltage of 1.0 V. The drain voltage is fixed to be 10 mV. Uniform trap density in energy and space is assumed. The distribution width of the noise contribution is about $4k_B T \approx 0.1$ eV.

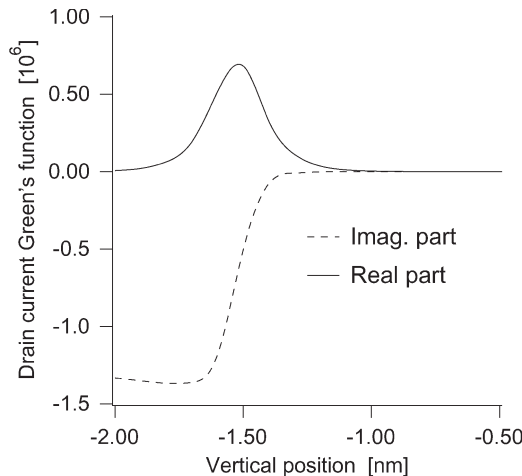


Fig. 8. Drain current Green's function for the oxide trap continuity equation in the "oxide trap region" at the gate voltage of 1.0 V and at 10 Hz. For this trap level, the energy difference from the electron quasi-Fermi energy is zero. The drain voltage is fixed to be 10 mV. The Si-SiO₂ interface is located at the zero vertical position. The value for the uniform trap distribution is shown.

spectral density of the drain noise current shows a very small value. The difference of the noise level between two parameter sets, which is prominent in the higher V_{GS} region, can be understood from the difference of the oxide trap density near the conduction band.

In Fig. 7, the contribution of each trap to the drain noise is shown. The trap levels whose E_t 's are close to the electron quasi-Fermi level contribute to the drain noise significantly. Therefore, for the small-signal noise analysis, it can be justified to consider the trap levels around the electron quasi-Fermi level only. Fig. 8 shows the drain current Green's function for the oxide trap continuity equation in the "oxide trap region." The gate voltage is 1.0 V, the drain voltage is 10 mV, and the observation frequency is 10 Hz. In Fig. 8, the oxide traps whose energy levels in the energy band diagram coincide with the electron quasi-Fermi energy at the interface are chosen. Both the noise source [the integrated γ in (9) and (10)] and the observation quantity (the terminal noise current) have the same

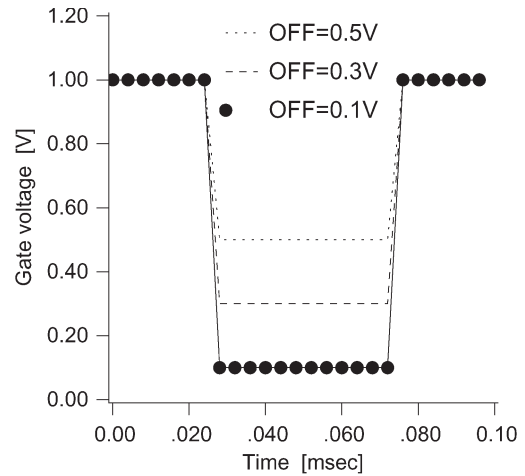


Fig. 9. Square-wave signal with 50% duty cycle applied to the gate terminal. The frequency of the square-wave signal is 10 kHz. The ON voltage is 1.0 V, and the OFF voltage is changed from 0.9 to 0.1 V with 0.1-V interval. The drain voltage is fixed to be 10 mV.

unit; therefore, the terminal current Green's function is given by a unitless quantity. While the drain current Green's function for the oxide trap continuity shows a large magnitude due to the amplification effect (for example, on the order of 10^6 in Fig. 8), usually its magnitude for electron continuity is smaller than unity. Since their magnitudes show a huge difference, only the Green's function for the oxide-trapping model, although both transfer functions are considered in our simulation. The real part of Green's function represents the drain noise current whose phase is the same as g-r noise sources in the oxide traps.

B. LS Operation With Oxide-Trapping Model

Now we calculate the $1/f$ noise spectrum when the MOSFET is in the LS operation. We consider the simplest case of a periodically switched MOSFET. Since our aim is to simulate the experimental setup [2]–[4], the gate voltage is driven by a square-wave signal with 50% duty cycle, as shown in Fig. 9. The frequency of the square-wave signal is 10 kHz. The ON voltage is 1.0 V, and the OFF voltage is varied from 1.0 (dc) to 0.1 V. The transition regions between the ON and OFF voltages are introduced to avoid problems with harmonic balance simulation. The drain bias voltage is fixed to be 10 mV. The harmonic balance simulation for the periodic steady state is carried out including 24 harmonics plus dc, thus leading to 49 collocation points.

Since full noise analysis is performed, any (m, m') component of the sideband correlation matrix $S(mf_0 + f, m'f_0 + f)$ [17], [19] is available for the given sideband frequency f . Among the many components of the sideband correlation matrix, usually, the diagonal components correspond to the noise power spectral density measured in the experiments. In Fig. 10, the diagonal components of the sideband correlation matrix of the drain noise current are plotted up to the first harmonic. It is clearly seen that a certain amount of the oxide-trapping noise is up-converted from the baseband to the first harmonic. Since the baseband noise is of particular interest in these experiments

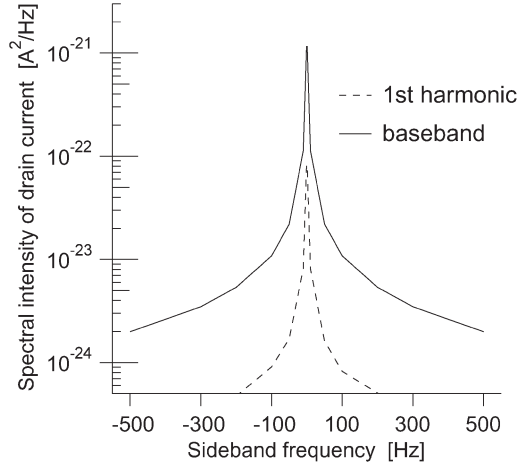


Fig. 10. Power spectral density up to the first harmonic. Simulated result for the U-shaped distribution is shown for the OFF voltage of 0.5 V. The center frequency of the first harmonic is 10 kHz.

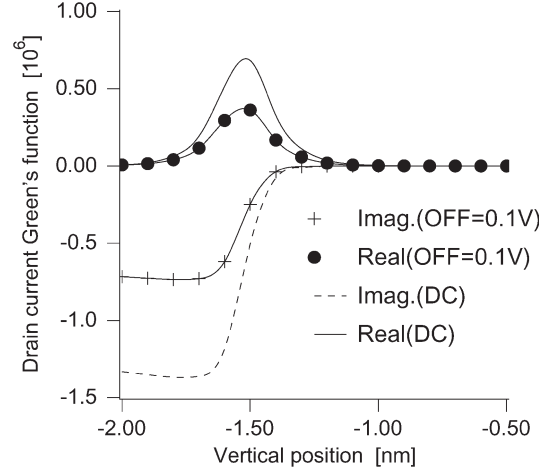


Fig. 12. Drain current conversion Green's functions for the oxide trap continuity equation in the "oxide trap region" at 10 Hz. The OFF voltage is 0.1 V.

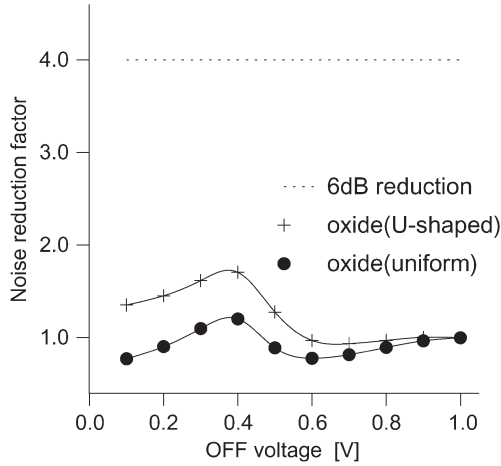


Fig. 11. Noise reduction factor for different OFF voltages. The small-signal $1/f$ noise model predicts 6-dB noise reduction.

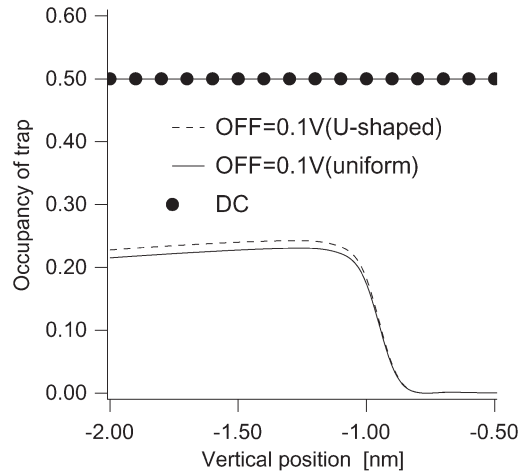


Fig. 13. Trap occupancy at 0.05 ms when the OFF voltage is 1.0 (dc) or 0.1 V. The trapped electron density in the oxide trap is reduced for the lower OFF voltages.

[2]–[4], in the following discussion, we concentrate on the noise characteristics in the baseband.

When the OFF voltage is v_{off} V, we define the noise reduction factor Γ_v as

$$\Gamma_v = \frac{S_{I_D, I_D}(\text{dc})}{S_{I_D, I_D}(\text{OFF} = v_{\text{off}})}. \quad (18)$$

Since the small-signal $1/f$ noise model predicts 6-dB noise reduction, the noise reduction factor should be 4. Fig. 11 shows the simulated noise reduction factor for different OFF voltages. When the trap distribution is uniform, the reduction factor of the drain noise current is close to unity. Its maximum value is at most 1.20 for the OFF voltage of 0.4 V. This is in strong contrast with the experimental results [2]–[4]. When the trap distribution is U-shaped, the reduction factor is slightly increased for all OFF voltages. However, its effect is not significant, although we adopt a reasonable value for the trap distribution. Therefore, the nonuniform distribution of the oxide trap in the energy space cannot explain the noise reduction over 6 dB properly, at least in this simulation.

To explain this result, the behavior of the internal quantities is investigated. In Fig. 12, the conversion Green's functions from baseband to baseband for the oxide trap continuity equation are shown for the dc case and the OFF voltage of 0.1 V. Since both trap distributions show quite similar results, the values for uniform distribution are shown. Among the 25 trap levels included in this simulation, the one that is exactly aligned with the electron quasi-Fermi level at the dc bias condition ($V_{\text{GS}} = 1$ V and $V_{\text{DS}} = 10$ mV) is chosen. In other words, this trap level is the biggest contributor to the drain noise current for the dc case. The conversion Green's function for the OFF voltage of 0.1 V is half of that for the dc case. Since the square of the conversion Green's function is involved with the output power spectral density, it means that a 6-dB noise reduction will be observed due to the reduced transfer function when we consider only this trap level. In Fig. 13, the trap occupancy of the same trap level at 0.05 ms is shown for the dc case and the OFF voltage of 0.1 V. Traps close to the interface (up to -0.8 nm in the figure) are almost empty because they can easily exchange electrons with the conduction band. Even in the case of traps

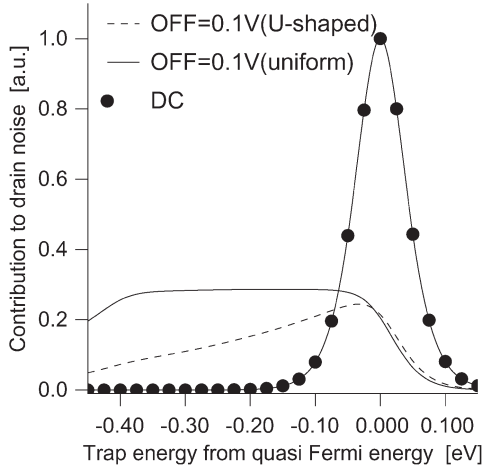


Fig. 14. Contribution to the power spectral density at 10 Hz from each trap level. Normalized values to the dc ones are shown.

located far from the interface, the trapped electron density in the oxide trap is significantly reduced for lower OFF voltage. Then, the power spectral density of the Langevin noise source is also reduced. Therefore, an additional noise reduction of over 6 dB will be observed due to the reduced trap occupancy when we consider only this trap level.

However, when we consider all trap levels, the above discussion is no longer valid. In Fig. 14, the contribution to the power spectral density from each trap level is shown. In the dc case, only the traps near the electron quasi-Fermi level contribute dominantly. However, in the switching case, the contribution is spread out over a wide range. In particular, traps that are fully filled in the dc case contribute significantly in the switching case. Under the LS operation, they are no longer fully occupied, so the transition between these trap levels and the conduction band is increased.

C. LS Operation With Hooge's Empirical Model

Using Hooge's empirical model, the same device has been simulated. At this time, the MOSFET is simulated without the oxide traps. For the sake of simplicity, we employ a constant Hooge's parameter 2.4×10^{-4} , which is found to generate the same noise power at the reference bias condition ($V_{GS} = 1.0$ V). Fig. 15 shows the noise reduction factor for different OFF voltages. Although the reduction factor of Hooge's model is larger than that of the oxide-trapping model, the additional noise reduction over the conventional 6-dB noise reduction is not observed even in this case either.

In Fig. 16, the conversion Green's functions from baseband to baseband for the electron continuity equation are shown for the dc case and the OFF voltage of 0.1 V. The relevant transfer function is the gradient of the conversion Green's function for the electron continuity equation. The gradient of the Green's function is slightly larger in the LS case than in the small-signal case. A slight decrease of the simulated reduction factor from the ideal value of 4 can be attributed to this change of relevant transfer function. Therefore, the modulation of Hooge's noise source plays an important role in $1/f$ noise reduction in this model.

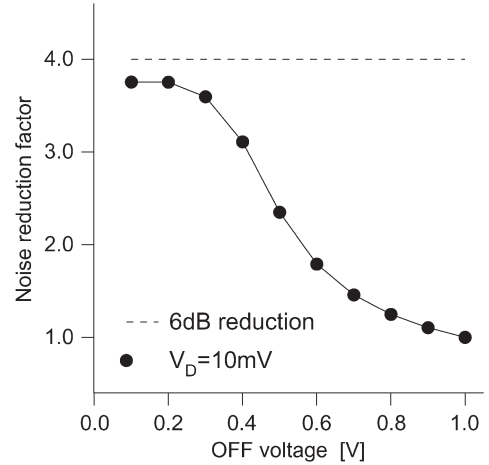


Fig. 15. Noise reduction factor for different OFF voltages when Hooge's empirical model is exploited. Hooge's parameter is assumed to be instantaneous.

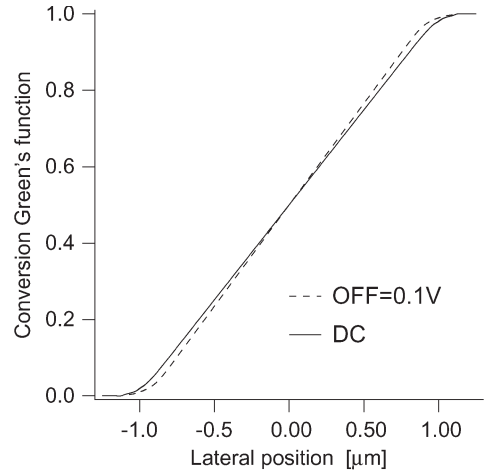


Fig. 16. Drain current conversion Green's function from baseband to baseband for the electron continuity equation. The drain voltage is 10 mV. Values at Si-SiO₂ are shown.

Hooge's noise source for switched MOSFET can be analyzed as follows. For the baseband frequency, the power spectral density of Hooge's noise source in (15) becomes

$$S_{\xi_n, \xi_n}(\mathbf{r}, \mathbf{r}', f, f) = |K_0(\mathbf{r})|^2 \frac{1}{f} \delta(\mathbf{r} - \mathbf{r}') I \quad (19)$$

where K_0 is the time average of the amplitude modulation over one period T_0 , i.e.,

$$K_0 = \frac{1}{T_0} \int_0^{T_0} \alpha_H(\mathbf{r}) \frac{|\mathbf{J}_{ns}(\mathbf{r})|^2}{n(\mathbf{r})} dt. \quad (20)$$

Since the current density almost vanishes in the OFF condition, if the gate voltage is driven by a square-wave signal with 50% duty cycle, then the expression for K_0 is simplified to

$$K_0 = \frac{1}{2} \alpha_{H, on}(\mathbf{r}) \frac{|\mathbf{J}_{ns, on}(\mathbf{r})|^2}{n_{on}(\mathbf{r})} \quad (21)$$

where the subscript *on* denotes the quantity at the ON condition. Therefore, the power spectral density of Hooge's noise source is reduced by 6 dB. Note that Hooge's parameter in the OFF

condition does not appear in the above expression. From this argument, we can conclude that Hooge's parameter for the MOSFET cannot be an instantaneous function to explain the experimental results of more than 6-dB noise reduction. Rather, it should contain information about the periodic device operation.

IV. CONCLUSION

The $1/f$ noise in MOSFETs under LS operation has been modeled by using both McWhorter's oxide-trapping model and Hooge's empirical model. In the oxide-trapping model, the contribution to noise power spectral density (PSD) of traps aligned to the electron quasi-Fermi level at the dc case was decreased by more than 6 dB. However, when the trap distribution was uniform, no significant reduction of the $1/f$ noise PSD under LS operation was observed. When the trap distribution was U-shaped, the noise reduction factor was increased, but its effect was not significant. In Hooge's model, an almost 6-dB noise decrease was observed for the low OFF voltages. It is the same result with that of the small-signal $1/f$ noise model. When Hooge's parameter for the MOSFET was an instantaneous function, we could not explain the additional decrease of noise. To explain the experimental results using this model, the noise source should depend not only on the instantaneous operating point but also on the periodic device operation over the whole period. In idealized cases, both models fall short of predicting more than 6-dB decrease of $1/f$ noise PSD in MOSFETs under the LS condition.

ACKNOWLEDGMENT

The authors would like to thank Prof. C. Jungemann of Bundeswehr University (Germany) for supporting the computing resources.

REFERENCES

- [1] A. Hajimiri and T. H. Lee, "A general theory of phase noise in electrical oscillators," *IEEE J. Solid-State Circuits*, vol. 33, no. 2, pp. 179–194, Feb. 1998.
- [2] I. Bloom and Y. Nemirovsky, " $1/f$ noise reduction of metal–oxide semiconductor transistors by cycling from inversion to accumulation," *Appl. Phys. Lett.*, vol. 58, no. 15, pp. 1664–1666, Apr. 1991.
- [3] S. L. J. Gierkink, E. A. M. Klumperink, A. P. van der Wel, G. Hoogzaad, E. van Tuijl, and B. Nauta, "Intrinsic $1/f$ device noise reduction and its effect on phase noise in CMOS ring oscillators," *IEEE J. Solid-State Circuits*, vol. 34, no. 7, pp. 1022–1025, Jul. 1999.
- [4] A. P. van der Wel, E. A. M. Klumperink, S. L. J. Gierkink, R. F. Wassenaar, and H. Wallinga, "MOSFET $1/f$ noise measurement under switched bias conditions," *IEEE Electron Device Lett.*, vol. 21, no. 1, pp. 43–46, Jan. 2000.
- [5] H. Tian and A. E. Gamal, "Analysis of $1/f$ noise in switched MOSFET circuits," *IEEE Trans. Circuits Syst. II, Analog Digit. Signal Process.*, vol. 48, no. 2, pp. 151–157, Feb. 2001.
- [6] J. S. Kolhatkar, E. Hoekstra, C. Salm, A. P. van der Wel, E. A. M. Klumperink, J. Schmitz, and H. Wallinga, "Modeling of RTS noise in MOSFETs under steady-state and large-signal excitation," in *IEDM Tech. Dig.*, 2005, pp. 759–765.
- [7] F. C. Hou, G. Bosman, and M. E. Law, "Simulation of oxide trapping noise in submicron n-channel MOSFETs," *IEEE Trans. Electron Devices*, vol. 50, no. 3, pp. 846–852, Mar. 2003.
- [8] C.-Y. Chen, Y. Liu, R. W. Dutton, J. Sato-Iwanaga, A. Inoue, and H. Sorada, "Numerical study of flicker noise in p-type $\text{Si}_{0.7}\text{Ge}_{0.3}/\text{Si}$ heterostructure MOSFETs," *IEEE Trans. Electron Devices*, vol. 55, no. 7, pp. 1741–1748, Jul. 2008.
- [9] H. S. Fu and C. S. Sah, "Theory and experiments on surface $1/f$ noise," *IEEE Trans. Electron Devices*, vol. ED-19, no. 2, pp. 273–285, Feb. 1972.
- [10] F. N. Hooge, T. G. M. Kleinpenning, and L. K. J. Vandamme, "Experimental studies on $1/f$ noise," *Rep. Prog. Phys.*, vol. 44, no. 5, pp. 479–532, May 1981.
- [11] F. N. Hooge, " $1/f$ noise sources," *IEEE Trans. Electron Devices*, vol. 41, no. 11, pp. 1926–1935, Nov. 1994.
- [12] L. K. J. Vandamme and F. N. Hooge, "What do we certainly know about $1/f$ noise in MOSTs?" *IEEE Trans. Electron Devices*, vol. 55, no. 11, pp. 3070–3085, Nov. 2008.
- [13] L. K. J. Vandamme, X. Li, and D. Rigaud, " $1/f$ noise in MOS devices, mobility or number fluctuations?" *IEEE Trans. Electron Devices*, vol. 41, no. 11, pp. 1936–1945, Nov. 1994.
- [14] A. L. McWhorter, " $1/f$ noise and related surface effects in germanium," MIT Lincoln Lab., Lexington, MA, Tech. Rep. No. 80, 1955.
- [15] H. Nah, S.-M. Hong, Y. J. Park, and H. S. Min, "The physical and numerical implications of the noise modeling method: IFM, CPM, and ERS," in *Proc. Int. Conf. Simul. Semicond. Processes Devices*, 2003, pp. 75–78.
- [16] A. Demir and A. Sangiovanni-Vincentelli, *Analysis and Simulation of Noise in Nonlinear Electronic Circuits and Systems*. Norwell, MA: Kluwer, 1998.
- [17] F. Bonani, S. D. Guerrieri, G. Ghione, and M. P. Pirola, "A TCAD approach to the physics-based modeling of frequency conversion and noise in semiconductor devices under large-signal forced operation," *IEEE Trans. Electron Devices*, vol. 48, no. 5, pp. 966–977, May 2001.
- [18] F. Bonani, S. D. Guerrieri, and G. Ghione, "Noise source modeling for cyclostationary noise analysis in large-signal device operation," *IEEE Trans. Electron Devices*, vol. 49, no. 9, pp. 1640–1647, Sep. 2002.
- [19] F. Bonani, S. D. Guerrieri, and G. Ghione, "Physics-based simulation techniques for small- and large-signal device noise analysis in RF applications," *IEEE Trans. Electron Devices*, vol. 50, no. 3, pp. 633–644, Mar. 2003.
- [20] S.-M. Hong, R. Kim, C. H. Park, H. S. Min, and Y. J. Park, "A physics-based TCAD framework for the noise analysis of RF CMOS circuits under the large signal operation," in *Proc. Int. Conf. Simulation Semiconductor Processes Devices*, 2005, pp. 119–122.
- [21] S.-M. Hong, C. H. Park, H. S. Min, and Y. J. Park, "Physics-based analysis and simulation of phase noise in oscillators," *IEEE Trans. Electron Devices*, vol. 53, no. 9, pp. 2195–2201, Sep. 2006.
- [22] K. S. Kundert, "Introduction to RF simulation and its application," *IEEE J. Solid-State Circuits*, vol. 34, no. 9, pp. 1298–1319, Sep. 1999.
- [23] O. Nastov, R. Telichevsky, K. Kundert, and J. White, "Fundamentals of fast simulation algorithms for RF circuits," *Proc. IEEE*, vol. 95, no. 3, pp. 600–621, Mar. 2007.
- [24] B. Troyanovsky, "Frequency domain algorithms for simulating large signal distortion in semiconductor devices," Ph.D. dissertation, Stanford Univ., Stanford, CA, 1997.
- [25] F. M. Rotella, G. Ma, Z. Yu, and R. W. Dutton, "Modeling, analysis, and design of RF LDMOS devices using harmonic balance device simulation," *IEEE Trans. Microw. Theory Tech.*, vol. 48, no. 6, pp. 991–999, Jun. 2000.
- [26] Y. Hu and K. Mayaram, "Periodic steady-state analysis for coupled device and circuit simulation," in *Proc. Int. Conf. Simul. Semicond. Processes Devices*, 2000, pp. 90–93.
- [27] J. E. Sanchez, G. Bosman, and M. E. Law, "Two-dimensional semiconductor device simulation of trap-assisted generation-recombination noise under periodic large-signal conditions and its use for developing cyclostationary circuit simulation models," *IEEE Trans. Electron Devices*, vol. 50, no. 5, pp. 1353–1362, May 2003.
- [28] G. Ghione, F. Bonani, S. Donati, F. Bertazzi, and G. Conte, "Physics-based noise modelling of semiconductor devices in large signal operation including low-frequency noise conversion effects," in *IEDM Tech. Dig.*, 2005, pp. 212–215.
- [29] M. Bollhöfer and Y. Saad, *ILUPACK—Preconditioning Software Package*. [Online]. Available: <http://www-public.tu-bs.de/~bolle/ilupack/>
- [30] M. N. Darwish, J. L. Lentz, M. R. Pinto, P. M. Zeitzoff, T. J. Krutsick, and H. H. Vuong, "An improved electron and hole mobility model for general purpose device simulation," *IEEE Trans. Electron Devices*, vol. 44, no. 9, pp. 1529–1538, Sep. 1997.
- [31] Z. Celik and T. Y. Hsiang, "Study of $1/f$ noise in n-MOSFETs: Linear region," *IEEE Trans. Electron Devices*, vol. ED-32, no. 12, pp. 2797–2802, Dec. 1985.
- [32] Z. Celik-Butler and T. Y. Hsiang, "Spectral dependence of $1/f^\gamma$ noise on gate bias in n-MOSFETs," *Solid State Electron.*, vol. 30, no. 4, pp. 419–423, Apr. 1987.
- [33] A. P. van der Wel, E. A. M. Klumperink, J. S. Kolhatkar, E. Hoekstra, M. F. Snoeij, C. Salm, H. Wallinga, and B. Nauta, "Low-frequency noise phenomena in switched MOSFETs," *IEEE J. Solid-State Circuits*, vol. 42, no. 3, pp. 540–550, Mar. 2007.



Sung-Min Hong (M'08) was born in Korea, in 1978. He received the B.S. degree in electrical engineering and the Ph.D. degree in electrical engineering and computer science from Seoul National University, Seoul, Korea, in 2001 and 2007, respectively.

He was a Postdoctoral Researcher with the Nano Systems Institute, Seoul National University, until June 2007. Since August 2007, he has been a Postdoctoral Research Associate with the Institute for Microelectronics and Circuit Theory (EIT4), Bundeswehr University, Neubiberg, Germany. His current research interests include the development of a deterministic Boltzmann equation solver based on the spherical harmonic expansion and the noise modeling in semiconductor devices.



Chan Hyeong Park (S'00–M'00) was born in Hong Seong, Korea, in 1970. He received the B.S., M.S., and Ph.D. degrees in electronics engineering from Seoul National University, Seoul, Korea, in 1992, 1994, and 2000, respectively.

From 2000 to 2003, he was a Visiting Scientist with the Research Laboratory of Electronics, Massachusetts Institute of Technology (MIT), Cambridge. Since 2003, he has been with Kwangwoon University, Seoul, where he is currently an Associate Professor with the Department of Electronics and Communications Engineering. He is now on a sabbatical leave as a Visiting Scientist with MIT and is working on the modeling of new energy production phenomena in electrode–electrolyte systems. His current research interests include the modeling and simulation of noise processes in CMOS ICs and carrier transport in nanoscale devices.



Young June Park (S'77–M'83–SM'05) received the B.S. and M.S. degrees from Seoul National University (SNU), Seoul, Korea, in 1975 and 1977, respectively, and the Ph.D. degree from the University of Massachusetts, Amherst, in 1983.

From 1983 to 1985, he was with the Device Physics and Technology Department, IBM, East Fishkill, NY. In 1985, he was with Gold Star Semiconductor Company (currently Hynix Semiconductor Inc.), Anyang, China, where he worked in the area of CMOS technology. Since 1988, he has been with SNU, where he is currently a Professor with the School of Electrical Engineering and Computer Science. In 1993, he spent his sabbatical year at Stanford University, Stanford, CA, and performed research on advanced semiconductor transport modeling. From 1996 to 2001, he was the Director of the Inter-University Semiconductor Research Center (ISRC), SNU. In 2001, he was on a leave of absence to work for Hynix Semiconductor Inc. as Director of the Memory Research and Development Division. Since 2003, he has served as the Director of the Nano System Institute under the National Core Research Center (NCRC) program supported by the Korea Science and Engineering Foundation, Korea. His research interests include advanced device structures, device/noise and reliability modeling, low-power circuit technology, nano MOSFET modeling, and MOSFET applications to bio-systems.



Hong Shick Min received the B.S. degree in electronics engineering from Seoul National University (SNU), Seoul, Korea, in 1966, and the M.S. and Ph.D. degrees in electrical engineering from the University of Minnesota, Minneapolis, in 1969 and 1971, respectively.

From 1971 to 1972, he was a Postdoctoral Fellow with the University of Minnesota. In 1973, he was an Assistant Professor with the Department of Electronics Engineering, Korea University, Seoul. Since 1976, he has been with the School of Electrical Engineering, SNU, where he is currently a Professor. His main research interests include noise in semiconductors and semiconductor devices.